Universality class of absorbing transitions with continuously varying critical exponents

Jae Dong Noh
Department of Physics, Chungnam National University, Daejon 305-764, Korea

Hyunggyu Park
School of Physics, Korea Institute for Advanced Study, Seoul 130-012, Korea

(Received 2 December 2002; revised manuscript received 30 September 2003; published 30 January 2004)

The well-established universality classes of absorbing critical phenomena are directed percolation (DP) and directed Ising (DI) classes. Recently, the pair contact process with diffusion (PCPD) has been investigated extensively and claimed to exhibit a different type of critical phenomenon distinct from both DP and DI classes. Noticing that the PCPD possesses a long-term memory effect, we introduce a generalized version of the PCPD (GPCPD) with a parameter controlling the memory strength. The GPCPD connects the DP fixed point to the PCPD point continuously. Monte Carlo simulations strongly suggest that the GPCPD displays, to our knowledge, novel critical phenomena which are characterized by continuously varying critical exponents. The same critical behaviors are also observed in models where two species of particles are coupled cyclically. We present one possible scenario that the long-term memory may serve as a marginal perturbation to the ordinary DP fixed point.

DOI: 10.1103/PhysRevE.69.016122 PACS number(s): 64.60.Ht, 05.70.Ln

I. INTRODUCTION

A nonequilibrium system with trapped (absorbing) states may display a so-called absorbing phase transition between an inactive and an active phase [1,2]. A state which has a zero transition probability into any other state is called the absorbing state. A system in the inactive phase always evolves into the absorbing state and stays there forever. On the other hand, a system in the active phase may not be trapped in the absorbing state with a finite probability. There has been growing interest in the critical behaviors of the absorbing phase transitions since a wide range of phenomena such as epidemic spreading, catalytic chemical reactions, and surface roughening, display absorbing transitions [1,2].

Besides their wide applications, absorbing critical phenomena have been the focus of a number of theoretical works, since they are categorized into a few universality classes characterized by the symmetry between the absorbing states and/or the conservation in dynamics [3–6]. Criticality of each universality class is described by three independent critical exponents; β for the order parameter, $\nu_\perp$ for the correlation length, and $\nu_\parallel$ for the relaxation time. For systems which are free from quenched disorder and evolve only through short-range processes, the directed percolation (DP) and the directed Ising (DI) (or parity conserving) classes are well-established ones.

The DP class involves typically a single absorbing state without any kind of conservation in dynamics [7,8]. The contact process, a model for epidemic spreading, is a prototypical example of the DP class [9]. In this model, individuals on a lattice are either infected or healthy. Infected ones may be healed spontaneously or infect healthy neighbors. There is a single absorbing state where all individuals are healthy. Varying the relative rates between infection and healing processes, one can find a phase transition from the absorbing phase into the active phase.

Its stationary and dynamic critical behaviors are characterized by spatiotemporal cluster patterns of infected individuals. These clusters can be mapped to the directed percolation clusters [1], when the temporal direction is set to be the preferred direction of DP clusters. So all critical exponents (fractal dimensions) take the same values as the corresponding DP critical exponents. Most of the systems with absorbing states belong to this DP class, e.g. the Domany-Kinzel cellular automaton [10], the Ziff-Gulari-Barshad model for a surface catalytic reaction [11], the branching-annihilating random walks with an odd number of offspring [12], and the pair contact process (PCP) [13]. Unlike others, the PCP has infinitely many absorbing states, which leads to controversial transient behaviors, i.e., nonuniversal scaling [13–16] versus absence of scaling [17,18]. But its stationary critical behavior still belongs to the DP class at low dimensions [19].

The DI class includes systems with two equivalent absorbing states with Ising-like Z_2 symmetry or equivalently in one dimension (1D) a single absorbing state with parity conservation in the domain wall language. The nonequilibrium kinetic Ising (NKI) model with combined zero-temperature spin-flip dynamics and infinite-temperature spin-exchange dynamics is an example of the DI systems [20]. In this model, only Ising spins near domain walls can flip, so that the two states with all spins up or down are absorbing. These two absorbing states are probabilistically equivalent. In terms of the domain wall, there is a single absorbing state (vacuum) with parity conservation in the number of domain walls, since spin flips change it only in pairs. Other examples in the DI class include the interacting monomer-dimer model [21], the branching-annihilating random walks with an even number of offspring [12,22], and generalized versions of the contact process [5,23]. There also exist models in the DI universality class that have infinitely many absorbing states [24–26]. They also display nonuniversal scaling behaviors in the transient regime [25,26].

There is an *infinite dynamic barrier* between two absorbing states of DI systems, which is similar to the free energy barrier between two ground states in the ordered phase of the

equilibrium Ising system [24]. A state near one absorbing state cannot evolve into a state near the other absorbing state by a finite number of successive local changes. In other words, a frustration (domain wall) in a configuration generated by pasting two absorbing configurations cannot disappear within a finite number of time steps. For example, a spin state in the 1D NKI model with all spins up in one semi-infinite lattice and all spins down in the other semi-infinite lattice never relaxes to the absorbing state.

The concept of the infinite dynamic barrier is very useful to understand the critical behavior of systems with infinitely many absorbing states. For instance, the PCP [13] and the modified interacting monomer-dimer (IMD-IMA) model [24] have infinitely many absorbing states. In the PCP, a frustration between any of the absorbing states can disappear locally, so the absorbing transition falls into the DP class. However, in the IMD-IMA, the infinite dynamic barrier separates the absorbing states into two equivalent groups of absorbing states, which results in the DI-type critical behavior [24].

A few exceptional cases have been reported: Lévy-type long-range flights are relevant to the absorbing critical phenomena, which lead to continuous variation of critical exponents [27]. Multispecies particle reaction-diffusion systems also show non-DP and non-DI critical behaviors, where an interspecies hard-core interaction plays an important role [28]. A lattice gas model with a global conservation in the particle number shows a novel type criticality related to self-organized critical systems [29]. The nonequilibrium q-state Potts models in higher dimensions show interesting critical behaviors [30]. A quenched randomness also leads to different absorbing critical phenomena [31].

Recently, Howard and Täuber introduced a modified PCP (called as PCPD) model, which allows single-particle diffusion [32,33]. They studied the PCPD in the context of bosonic field theory and showed that the field theory is nonrenormalizable and the absorbing transition does not belong to the DP class. A fermionic version was first studied by Carlon, Henkel, and Schollwöck [34] in 1D, which raises continuing debate on the universality class [34–40]. Hereafter, we only focus on the 1D systems.

The PCPD is defined on a lattice, each site of which is either occupied by a particle (X) or empty ($\varnothing$). Dynamic rules are given as follows. A nearest neighbor pair of particles can either annihilate ($XX \rightarrow \varnothing\varnothing$) with probability $p(1-d)$ or branch one offspring ($XX \rightarrow XXX$) to one of the neighboring sites with probability $(1-p)(1-d)$. A particle can hop to its neighboring site with probability d. Branching and hopping attempts are rejected if a particle would land on the top of another particle.

When the diffusion is not allowed ($d=0$), it reduces to the ordinary PCP with infinitely many absorbing states. Any state with only isolated particles is an absorbing state. But there is no infinite dynamic barrier between them and the transition belongs to the DP class [13].

At nonzero d, the PCPD has only *two* absorbing states; a vacuum state and a state with a single diffusing particle. In fact, the latter forms an absorbing subspace consisting of L configurations with system size L in 1D. Once the system evolves into this absorbing subspace, it drifts freely inside the subspace but cannot escape out of it. The threshold transfer process [15] is one example with an absorbing subspace. But it does not contain any other absorbing state and displays the DP-type transition.

The structure of absorbing states in the PCPD is unique with one pointlike absorbing state and one absorbing subspace. It is clear that there is no infinite dynamic barrier between these absorbing states. Hence, one may argue that the PCPD should belong to the DP class. However, this argument turns out to be premature. Background diffusing solitary particles generate a *long-term memory effect* on the order parameter (pair density). Solitary particles detached from different trains of particles diffuse and collide each other to create a new particle pair, which leads to history dependence in the pair-creation rate. This process is governed by annihilating random walks, where the colliding probability of two walkers decays algebraically with time. This long-term memory effect might be relevant and leads to a new type of critical phenomenon.

A numerical investigation using density matrix renormalization group techniques [34] revealed that numerical values of some critical exponent ratios are close to the DI values rather than the DP values. Subsequent extensive simulations [35–37] seem to exclude the possibility of both DI and DP classes and suggest that the PCPD belongs to a new universality class. However, huge corrections to scaling conceal the true asymptotic scaling behavior and numerical estimates for the critical exponents are obscure with considerable uncertainty. Similar critical behaviors were also observed in related models [38–40], which include a modified PCPD [39] with the branching process $2X \rightarrow 4X$ instead of $2X \rightarrow 3X$ and an effective model with two species of particles coupled cyclically [38].

Despite all those efforts, universal features that could characterize the novel universality class were not uncovered yet. We explore this issue in the present work. Hinrichsen noticed that two types of degrees of freedom are present in the PCPD; a particle pair that can branch and annihilate, and a diffusing solitary particle [38]. All activities that can change the number of particles are carried out by the particle pairs. So the particle pair density can be regarded as an order parameter. The two degrees of freedom are coupled cyclically; one can be transmuted to the other, and vice versa, via particle diffusion. The cyclic coupling results in the long-term memory effect as described above, which we believe plays a crucial role in this critical phenomenon.

These observations lead us to consider a generalized PCPD (GPCPD) model with a parameter controlling the strength of the memory effect, which will be explained in Sec. II. Without the memory effect, the GPCPD should fall into the DP class. So, our parameter connects the DP fixed point to the PCPD point, which allows us to study the long-term memory effect on the DP-type models systematically.

One may expect that the long-term memory would serve as a relevant (at least, marginal) perturbation to the DP fixed point, in order to account for the non-DP-type novel critical behavior at the PCPD point. In that case, one can hope that, by varying the control parameter, those huge corrections to

scaling found at the PCPD point might be reduced to a tolerable level, so the moderate numerical efforts may reveal the true asymptotic behavior.

We performed extensive Monte Carlo simulations in Sec. III. Our numerical results show that corrections to scaling are huge only near the PCPD point and the asymptotic regimes are rather easily reached at other values of the control parameter. So, we were able to estimate the values of the critical exponents with reasonable accuracy for a wide range of the control parameter, except not very near the PCPD point. In the absence of the memory effect, we find the DP universality class as expected. With the memory effect, surprisingly, we observe continuous variation of critical exponents with the memory strength. Especially, the order parameter exponent β varies more than 60%, which is far beyond the statistical errors less than at most 10%.

In order to establish this novel universality class with continuously varying critical exponents firmly, in Sec. IV, we introduce two independent model systems with two species of particles: one species plays the role of the particle pairs and the other the role of the diffusing solitary particles. They are coupled cyclically through transmutations, which leads to the long-term memory effect. These models are also studied by Monte Carlo simulations, and are shown to display the same type of critical phenomena as in the GPCPD.

In Sec. V, we suggest one possible scenario to account for this universality class with continuously varying exponents. This scenario assumes that the long-term memory plays the role of the marginal perturbation to the DP fixed point. We numerically check this scenario by measuring the lifetime distribution of solitary particles. Our analysis shows that this scenario may be considered as a reasonable one, though it needs full field-theoretical analysis for a definitive test. Finally, in Sec. VI, we summarize our works and discuss over various possible scenarios recently suggested by other researchers.

II. MODEL

The GPCPD model is defined on a 1D lattice of size L with the periodic boundary conditions. Each site is either occupied by a particle (X) or empty ($\varnothing$). The system evolves in time according to the dynamic rules of the PCPD (see Sec. I) with one additional ingredient. When the hopping of a solitary particle creates a new particle pair through colliding with another particle, this new particle pair annihilates instantaneously with probability $1-r$ or survives with probability r. This does not apply to particle pairs formed by branching processes. At $r=0$, two solitary particles always annihilate upon meeting and have no chance to turn into a nearest neighbor particle pair. The parameter r controls the transmutation rate of two solitary particles into a nearest neighbor particle pair upon meeting. At $r=1$, the model reduces to the ordinary PCPD.

As in the PCP, we take the particle pair density as the order parameter. At nonzero r, there is a feedback mechanism to increase the pair density via the collision of diffusing solitary particles. A solitary particle is created from a train of particles by a hopping (detaching) process of a boundary particle or a pair annihilation process of a triplet of particles. In this process, at least one particle pair is sacrificed. The solitary particles diffuse and collide with each other to form a particle pair with probability r. So, one can say that particle pairs temporarily turn into solitary particles and resurrect later by collision of those solitary particles. The colliding probability of two diffusing particles usually decays algebraically in time. Therefore, this feedback mechanism induces long-term history dependence, which is called the *long-term memory effect*, of the order parameter. As r increases, the long-term memory effect becomes stronger. The PCPD model ($r=1$) has the maximum memory effect.

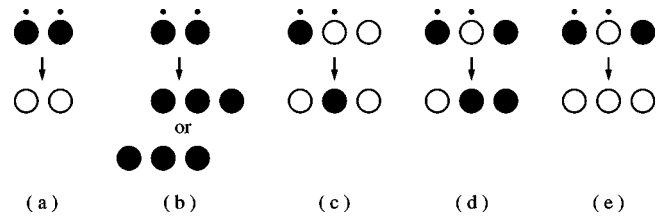

FIG. 1. Illustration of dynamic rules. Filled (empty) circles represent occupied (empty) sites. Dots indicate selected sites.

The $r=0$ point is special. Collision of two particles does not generate a particle pair at all, so there is no feedback mechanism for the pair density. Once the system evolves into a state without any particle pair, it stays inside a subspace of states without a pair and, in the end, will be trapped into one of the absorbing states (the vacuum state and the states with a single particle). So, in the viewpoint of the order parameter as the pair density, the no-pair subspace serves as the absorbing subspace which the system cannot escape from. Evolution inside this subspace is governed by the trivial pair annihilation dynamics of diffusing particles that have no memory effects on the order parameter fluctuations. Therefore, the GPCPD at $r=0$ should be effectively equivalent to the PCP model without diffusion. The no-pair subspace is exactly the same as the absorbing subspace of the latter. The coupling constants for the branching and annihilation processes are renormalized due to the inclusion of the single-particle diffusion, and the critical point is shifted. However, the critical fluctuations should be identical and we expect the DP-type stationary critical behavior at the absorbing transition. We also expect the ordinary DP-type scaling in the transient regime, starting from a single pair of particles, in contrast to the controversial transient behaviors in the PCP model.

At nonzero r, the system escapes from the no-pair subspace with finite probability. The order parameter can be significantly influenced by the memory effect induced by this in-and-out dynamics with respect to the no-pair subspace. The parameter r connects the DP fixed point ($r=0$) to the PCPD point ($r=1$). Therefore, the GPCPD allows us to study systematically the origin of the new type of critical behavior found in the PCPD.

Dynamics of the GPCPD can be implemented in Monte Carlo simulations as follows (see Fig. 1). First, select a pair of sites $(i,i+1)$ at random. When both sites are occupied, the two particles (a) annihilate with probability $(1-d)p$ or (b) branch a particle at one of the neighboring sites, $i-1$ or $i+2$, with probability $(1-d)(1-p)$. Branching attempt to

an already occupied site is rejected. When only one site is occupied, (c) the particle hops to the other site with probability d. If the hopping (not branching) creates a new particle pair, the pair (d) survives with probability r or (e) annihilates with probability $1-r$. When both sites are empty, no change is made. The time increases by one unit after L such trials.

To speed up simulations, we adopted a technique utilizing a list of active pairs of neighboring sites. A neighboring site pair is stored in the active pair list if it contains at least one particle. Then, a site pair in the list is selected randomly for dynamics. The time increases by $1/N_{\text{pair}}$ with N_{pair} the number of active pairs in the list at each attempt.

III. MONTE CARLO SIMULATIONS

Monte Carlo simulations were performed to investigate critical behaviors of the GPCPD. The critical points are approached by varying p at each $r=0$, 0.25, 0.5, 0.75, and 1 with fixed diffusion probability $d=0.1$.

A. Defect simulations

We performed the so-called defect simulations to locate the critical points. Starting with a single pair of particles, we measured the survival probability $P(t)$ that the system is *surviving* at time t, the number of particle pairs $N(t)$ averaged over all samples, and the mean distance of spreading $R(t)$ averaged over the surviving samples.

Our definition of surviving samples is different from the conventional one where all samples not being trapped into one of the absorbing states are considered as surviving ones. Here, only samples with at least one particle pair are regarded as surviving. Samples with only solitary diffusing particles (no pair but irrespective of the number of particles) are regarded as *dead* ones, even if they are not trapped completely. They may be dead for a while, but can resurrect later as surviving samples when diffusing particles meet and form a particle pair. The dead states form the no-pair subspace (see Sec. II). At nonzero r, the system can evolve in and out of the no-pair subspace. With this definition, the survival probability $P(t)$ actually represents the probability that the system contains at least one particle pair, or equivalently the probability that the system stays outside the no-pair subspace.

The conventional surviving ensemble includes most of the states inside the no-pair subspace except the *true* absorbing states (the vacuum state and the states with a single particle). The survival probability is now dominated by the trivial pair-annihilation dynamics of diffusing particles inside the no-pair subspace [41], which does not reflect the proper dynamic and stationary scaling behavior of the order parameter (the pair density). Hence, the fluctuations of the order parameter should be described in our surviving ensemble defined as the complement of the no-pair subspace.

At criticality, the values of the measured quantities decay algebraically [42] as

$$P(t)\sim t^{-\delta'},$$

$$N(t)\sim t^{\eta}, \tag{1}$$

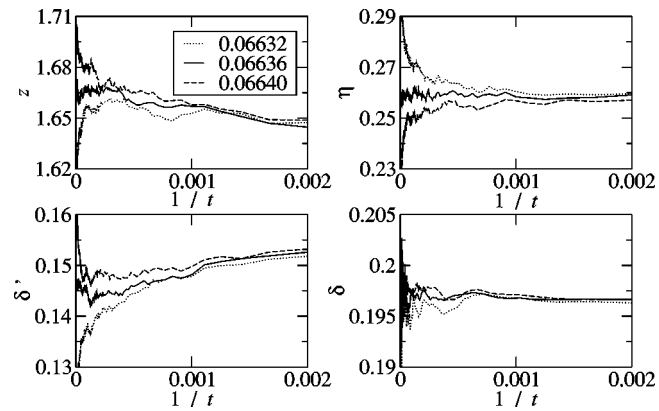

FIG. 2. The effective exponents for the GPCPD at $r=0.5$.

$$R(t)\sim t^{1/z},$$

and the double logarithmic plots against time show straight lines. Off criticality, these plots show curvatures in the long time limit. Precise estimates for the critical points and the scaling exponents can be obtained by examining the local slopes of the curves. The local slope, called as the effective exponent, is defined as

$$\delta'(t)=-\frac{\ln[P(t)/P(t/m)]}{\ln m},$$

and similarly for $\eta(t)$ and $z(t)$ with a constant m (taken to be 10). The power-law scaling behavior implies that they converge to the values of δ', η, and z asymptotically as $t\to\infty$ at $p=p_c$. At off-critical points, they behave like being at the critical point in the early time regime and then deviate to a trivial value characteristic of the active or inactive phase. From this crossover behavior one can determine the location of the critical point.

The defect simulations were performed up to 10^5 time steps and the observables were measured and averaged over $\sim 2\times 10^5$ samples. Figure 2 shows plots of the effective exponents against $1/t$ at $r=0.5$. Apparently, the effective exponents for δ', η, and z converge to their asymptotic values at $p=0.066\,36$, while they clearly bend up or down with a curvature at $p=0.066\,32$ and $0.066\,40$. It leads us to estimate that $p_c=0.066\,36(4)$ and $z=1.67(3)$, $\eta=0.26(1)$, $\delta'=0.14(1)$.

The errors in the exponent values mainly stem from the uncertainty in the p_c estimate. Statistical errors are much smaller than this systematic error, which can be clearly seen in Fig. 2. A correction to the scaling could lead to a systematic error in the estimate of p_c, and hence, of critical exponents. The plots in Fig. 2 show that the correction is quite small for $N(t)$. The effective exponents $\delta'(t)$ and $z(t)$ have a little time dependence (seemingly, linear dependence in $1/t$) even at the estimated p_c, while such time dependence is negligible for $\eta(t)$ at the estimated p_c. So the best estimate for p_c is obtained from the plot of $\eta(t)$ versus $1/t$ [43]. We also find similar behaviors for other values of r except $r=1$.

TABLE I. Critical points and critical exponents estimated from the defect simulations. As a reference, corresponding values of the DP and DI classes (taken from Ref. [22]) are given.

r	p_c	z	η	δ'	δ
0	0.04687(2)	1.58(1)	0.314(6)	0.160(5)	0.160(5)
0.25	0.05505(5)	1.62(3)	0.29(1)	0.15(1)	0.175(5)
0.50	0.06636(4)	1.67(3)	0.26(1)	0.14(1)	0.197(5)
0.75	0.08315(5)	1.75(5)	0.20(2)	0.13(2)	0.235(5)
1	0.1112(1)	1.7(1)	0.18(5)	0.09(2)	0.31
DP		1.579(2)	0.3137(10)	0.1596(4)	0.160(2)
DI		1.753(3)	0.000(1)	0.285(2)	0.285(4)

We also plot the combination of the effective exponents $\delta(t) \equiv 1/z(t) - [\eta(t) + \delta'(t)]$. At criticality, this exponent should converge asymptotically to the ratio of two stationary scaling exponents, $\beta/\nu_\parallel$ (known as the initial slip exponent), if the hyperscaling relation [15] is satisfied. At $r=0.5$, we obtain that $\delta = 0.197(5)$. This value will be compared to $\beta/\nu_\parallel$ estimated independently later in the static Monte Carlo simulations. The same analysis is repeated for other values of r and the results are summarized in Table I.

The two exponents δ and δ' do not necessarily coincide unless the evolution operator is invariant under the time-reversal transformation [2]. However, it is well known in models with multiple absorbing states that these two exponents coincide if one starts with the so-called *natural* initial configurations in defect simulations. This aspect will be discussed in details elsewhere [44].

The PCPD point at $r=1$ is an exceptional case. Very strong corrections to scaling are observed in all quantities as can be seen in Fig. 3. It has been already noted in Refs. [35,36]. We tried to locate the critical point from the curvature change in the plots of the effective exponent versus $1/t$. The plot of $\eta(t)$ versus $1/t$ shows that $p_c \simeq 0.1113$, while the plot of $\delta'(t)$ versus $1/t$ shows that $p_c \simeq 0.1112$. It suggests that the asymptotic scaling regime has not been reached yet until 10^5 time steps at the PCPD point. The exponent δ shows the worst behavior. Even one cannot see any difference between supercritical and subcritical behaviors (so we could not estimate an error bar of δ). So the values of p_c and critical exponents at the PCPD limit contain the largest uncertainty. It may be quite interesting to investigate the origin and the nature of the unexpected huge corrections at the PCPD point, but we do not have any reasonable explanation at this moment.

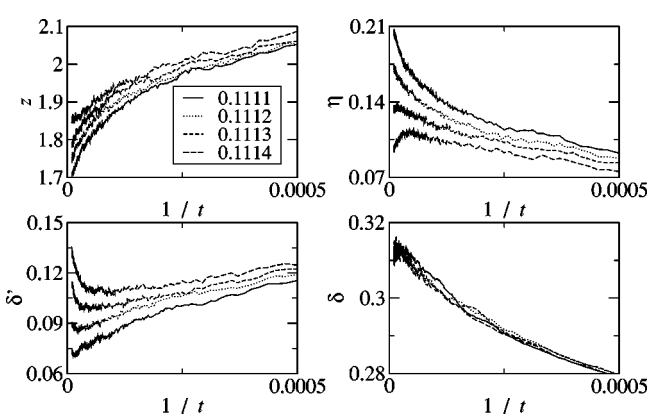

FIG. 3. The effective exponents for the PCPD ($r=1$).

When one faces a strong correction-to-scaling behavior in investigating numerically unknown critical phenomena of a model system, one may perform an extensive simulation up to much larger length scales and much longer time scales. However, if it is beyond the present day's computing capability, one should look for an efficient alternative model which presumably exhibits the same critical behavior with smaller correction to scaling. The PCPD model applies to such a case.

The GPCPD model may serve as an efficient alternative model for the PCPD model. The $r=1$ (PCPD) point of the GPCPD model is not a *special point*; it possesses neither an additional symmetry nor conservation law, compared to other points for $0<r<1$. Only the strength of the long-term memory effect changes with r. One may guess that the GPCPD model with all nonzero r may belong to the same universality class as the PCPD model and hope that the corrections to scaling are controllable for small r. It turns out that the GPCPD model possesses much smaller corrections to scaling for $r<1$ (at least up to $r=0.75$). So the critical points are very accurately estimated and the critical exponents are determined with reasonable errors.

At $r=0$, the values of all exponents are in excellent accord with the DP values. It confirms the expectation that the GPCPD without the memory effect should belong to the DP class. For other values of $r \neq 0$, the exponent values begin to deviate from the DP values. They are also clearly different from the DI values. It confirms that the GPCPD with the long-term memory effect ($r \neq 0$) displays, to our knowledge, novel-type critical phenomena that do not belong to the DP or DI universality class. More importantly and very surprisingly, the exponent values show a dependence on r (see Table I). This opens up a new possibility that the universality class would be characterized by continuously varying critical exponents, i.e., not a fixed point but a fixed line parametrized by the memory strength r. This remarkable finding should be examined carefully whether it is also present in the scaling property of the steady states.

B. Static simulations

The criticality in the steady states is studied via the so-called static Monte Carlo simulations where one starts with a macroscopically occupied configuration on finite size lattices. Here, we start with the fully occupied configuration and use the periodic boundary conditions. As the order parameter, we measure the pair density $\rho_s(t)$ averaged over surviving samples that contain at least one particle pair at a given time t, or equivalently averaged over the complementary states to the no-pair subspace, as defined in the defect simulations previously. The averaged quantities over the conventional surviving ensemble would also describe the system properly in the early time regime, up to the time scale when the system typically enters into the no-pair subspace. However, since then, the trivial pair-annihilation dynamics of dif-

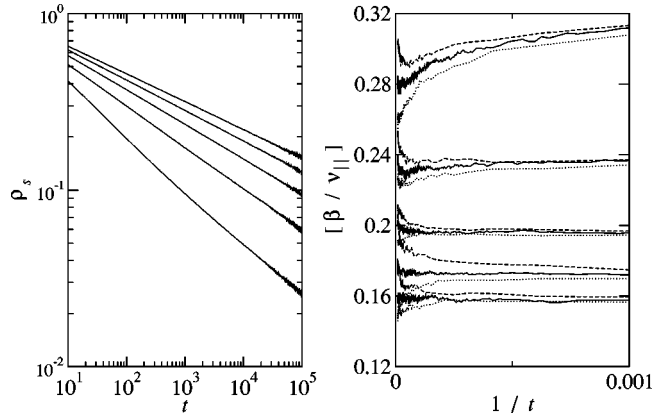

FIG. 4. Left: Order parameter decay at $p=p_c$ at each $r=0.0$ (top), . . . ,1.0 (bottom). Right: The effective exponent $[\beta/\nu_\parallel]$ defined with $m=8$. Solid lines represent the effective exponents at the estimated critical points (see text) and dotted (broken) lines at supercritical (subcritical) points at each $r=0.0$ (bottom), . . . ,1.0 (top).

fusing particles governs the system evolution [41] and the average value of the order parameter crosses over to the trivial stationary value.

The pair density averaged over our surviving ensemble satisfies a finite-size-scaling form as

$$\rho_s(\varepsilon,t,L)=L^{-\beta/\nu_\perp}f(\varepsilon L^{1/\nu_\perp},t/L^z), \tag{2}$$

where L is the system size and $\varepsilon\equiv p_c-p$ is the distance from the critical point p_c. The exponents β and $\nu_\perp$ are the critical exponents associated with the order parameter and the spatial correlation length, respectively. The dynamic exponent z is the ratio of the two exponents; $z=\nu_\parallel/\nu_\perp$, where $\nu_\parallel$ is the relaxation time exponent (see Ref. [2] for a review).

At criticality $(p=p_c)$, we have

$$\rho_s(0,\ t,L)=L^{-\beta/\nu_\perp}g(t/L^z)\ , \tag{3}$$

where $g(x)\sim x^{-\beta/\nu_\parallel}$ for small x and becomes a constant for large x. Thus, at $p=p_c$, the pair density decays as $\rho_s \sim t^{-\beta/\nu_\parallel}$ for $t\ll L^z$ and saturates to a steady-state value $\rho_s \sim L^{-\beta/\nu_\perp}$ for $t\gg L^z$.

The power-law scaling behavior in the transient regime $(t\ll L^z)$ can be studied with an effective exponent

$$[\beta/\nu_\parallel]\equiv-\frac{\ln[\rho_s(t)/\rho_s(t/m)]}{\ln m}$$

with a constant m. It converges to $\beta/\nu_\parallel$ for large t $(\ll L^z)$ at the critical point $p=p_c$, but deviates from it at $p\neq p_c$. Using this property we could determine the critical point p_c independently, and hence the exponent $\beta/\nu_\parallel$.

The order parameter is measured in a lattice of size $L=10^4$ up to $t=10^5$ time steps and averaged over 2000–5000 samples. The finite-size saturation effect is invisible up to $t=10^5$ for this system size. Figure 4 shows the log-log plots of the order parameter at the estimated critical points as well as the plots of the effective exponents at and near the criticality. From these plots, we estimate $p_c=0.046\,87(2)$, $0.055\,05(5)$, $0.066\,37(2)$, $0.083\,17(4)$, and $0.1113(1)$ at each value of $r=0$, 0.25, 0.5, 0.75, and 1, respectively. Except for the $r=1$ case, the values of the effective exponents at the estimated p_c do not show any significant systematic error and seem to reach their asymptotic values quite early, at around $t=10^3$. Statistical fluctuations are also very small. The off-critical data in Fig. 4 at the values of p displaced by the amount of error bars in the above p_c estimates clearly show either upward or downward curvatures, which demonstrates the accuracy of our p_c estimate. Moreover, these p_c values are in very good agreement with those obtained from the defect simulations (see Table I).

TABLE II. Critical exponents of the GPCPD and corresponding values of the DP and DI classes, taken from Ref. [22].

r	$\beta/\nu_\parallel$	$\beta/\nu_\perp$	z	$\nu_\perp$	β
0	0.159(1)	0.252(3)	1.58(1)	1.10(1)	0.277(5)
0.25	0.173(5)	0.282(5)	1.64(5)	1.10(3)	0.310(14)
0.50	0.197(3)	0.330(6)	1.69(5)	1.10(3)	0.363(17)
0.75	0.230(5)	0.40(1)	1.72(5)	1.17(5)	0.468(30)
1	0.27(4)	0.50(4)	1.8(2)	1.30(10)	0.65(12)
DP	0.1596(4)	0.2522(6)	1.5798(18)	1.0972(6)	0.2767(4)
DI	0.285(2)	0.500(5)	1.750(5)	1.84(6)	0.92(3)

The values of $\beta/\nu_\parallel$ are given by the limiting values of the effective exponents for large t at the estimated p_c, which are presented in Table II. For consistency, we use the defect simulation results for the p_c values and their errors. The estimated values of $\beta/\nu_\parallel$ are again in excellent accord with the values of $\delta=1/z-(\eta+\delta')$ measured in the defect simulations for $r\neq 1$, which implies that the hyperscaling relation [15] holds in this model.

Note that the correction to scaling is significant at the PCPD point $(r=1)$, as found in the defect simulations. At $r=1$, the effective exponent plot shows a strong time dependence even at the estimated critical point and there is a noticeable curvature in Fig. 4. It leads to a rather large error in the p_c estimate and, hence, the exponent estimates. Our estimate of $\beta/\nu_\parallel$ also shows a noticeable discrepancy with the estimate of δ (see Tables I and II). However, this discrepancy presumably comes from the inaccurate estimation of p_c at $r=1$ and insufficient time steps getting into the asymptotic regime. So it cannot be regarded as an evidence for the breakdown of the hyperscaling relation at the PCPD point.

The steady-state pair density for $t\gg L^z$ satisfies

$$\rho_s(\varepsilon,t=\infty,L)=L^{-\beta/\nu_\perp}h(\varepsilon L^{1/\nu_\perp}), \tag{4}$$

where the scaling function behaves as $h(x)\sim x^\beta$ for large x and becomes a constant near $x\simeq 0$. At criticality $(\varepsilon=0)$, it decays algebraically with size as $\rho_s\sim L^{-\beta/\nu_\perp}$. Utilizing this algebraic scaling property, we could also estimate the location of the critical points p_c. They again agree perfectly well with the previous other results.

We run 10^3–10^4 samples up to 4×10^6 time steps for the system size $L=2^6,\ldots,2^{11}$ at the estimated critical points given in Table I. Plots of ρ_s versus L at each critical point are

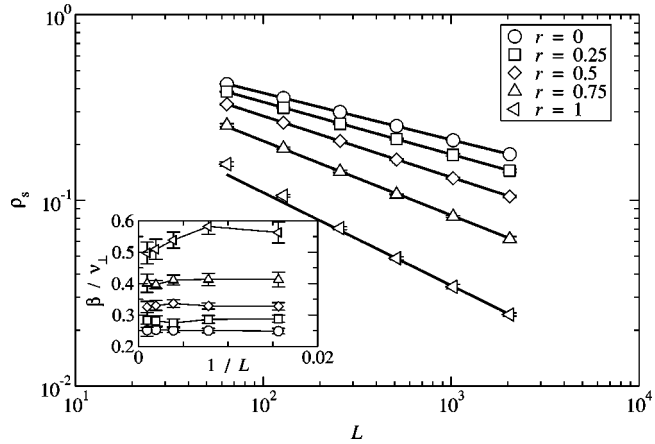

FIG. 5. The power-law scaling behavior of the order parameter at $p=p_c$ at each r. The solid line is a guide for the eyes whose slope is $\beta/\nu_\perp$ in Table II.

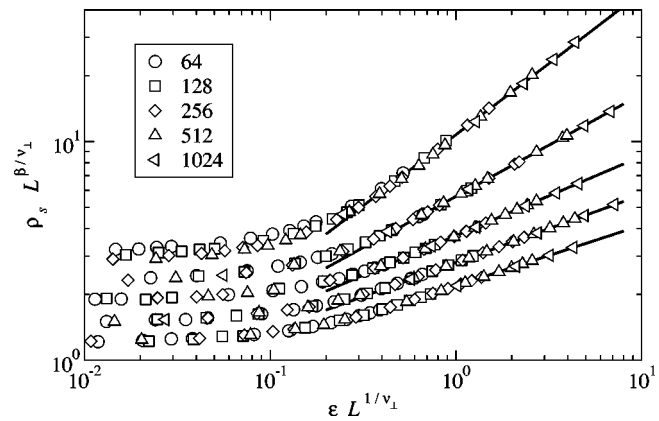

FIG. 7. Scaling plots according to Eq. (4) at each $r=0.0$ (bottom), . . . ,1.0 (top). The solid line is a guide for the eyes whose slope is β in Table II. Each dataset is shifted vertically by a constant factor to avoid an overlap with others at different values of r.

presented in Fig. 5. A least-squares straight-line fitting in the log-log plot might yield the value of $\beta/\nu_\perp$. However, it would result in an inaccurate estimate in the presence of a strong correction to scaling. Instead, we made use of an effective exponent $[\beta/\nu_\perp]=-\ln[\rho_s(2L)/\rho_s(L)]/\ln 2$ to extract the accurate exponent value from the extrapolation. It is plotted in the inset of Fig. 5 and the results are presented in Table II. As before, there exists a strong correction to the power-law scaling at the PCPD point at $r=1$, whereas such an effect is very small for the other values of r.

With p_c and $\beta/\nu_\perp$ determined, we could estimate the dynamic exponent z using the scaling form in Eq. (3). It was estimated as the optimal value that yields the best collapse of $\rho_s(\varepsilon=0,t,L)$ for $L=2^7,\ldots,2^{11}$ (see Fig. 6). The resulting values of z are presented in Table II. They are consistent with the ratio of the two exponent ratios, $\beta/\nu_\perp$ and $\beta/\nu_\parallel$, and agree very well with the values measured in the defect simulations.

We also determined the value of $\nu_\perp$ by collapsing off-critical steady-state data of $\rho_s(\varepsilon,t=\infty,L)$ in the scaling plot, using Eq. (4). In Fig. 7, the data for each r collapse well on a single curve with a specific value of $\nu_\perp$, respectively. The order parameter exponent β is then obtained by a product of $\beta/\nu_\perp$ and $\nu_\perp$ and presented in Table II. They are equal to the slopes of the scaling function $h(x)$ for large x in the log-log scale as shown in Fig. 7.

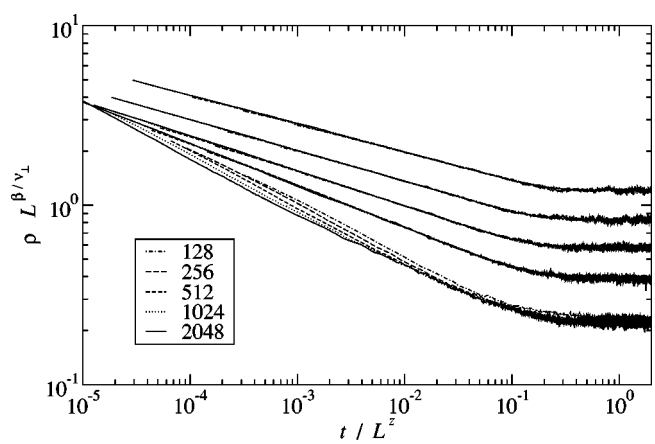

FIG. 6. Scaling plots according to Eq. (3) at each $r=0.0$ (top), . . . ,1.0 (bottom). Each dataset is shifted vertically by a constant factor to avoid an overlap with others at different values of r.

At the PCPD point ($r=1$), our results are consistent with those obtained by Carlon *et al.* [34] [$p_c=0.111(2)$, $z=1.87(3)$, and $\beta/\nu_\perp=0.50(3)$] and Hinrichsen [35] [$p_c=0.1112(1)$, $\beta/\nu_\parallel=0.25(2)$, $z=1.83(5)$, $\beta<0.67$]. Although some of critical exponent ratios are close to the DI values, the critical exponents are incompatible with those of the DI class. They are also inconsistent with the DP universality class. The strong correction-to-scaling behaviors were observed at the PCPD point with $r=1$ in both the defect and the static simulations. So our estimates for the critical exponents contain considerable uncertainty at the PCPD point. However, such corrections are not prominent for other values of r, which enables us to estimate the values of the critical exponents very accurately for $r<1$. As expected, the values of the critical exponents at $r=0$ agree very well with the DP values.

For $0<r<1$, the correlation length exponent $\nu_\perp$ seems to remain the same as the DP value for a wide range of r, at least up to 0.75. The value of the relaxation time exponent $\nu_\parallel=z\nu_\perp$ seems to increase slightly with increasing r (10% up to $r=0.75$), but, within present numerical accuracy, it may be difficult to conclude that its variation is real and not due to corrections to scaling. However, it is clearly visible that the order parameter exponent β (also $\beta/\nu_\perp$ and $\beta/\nu_\parallel$) varies considerably with r (more than 60%). It clearly signals a universality class with scaling exponents varying continuously with the parameter r.

Summing up all results, our Monte Carlo simulations show that the GPCPD displays the critical phenomena distinct from the DP and DI classes, with continuously varying exponents depending on the strength of the long-term memory effect r. These results are quite surprising and remarkable. In the renormalization group language, it implies

that there is a fixed line parametrized by r, instead of fixed points at two end points: the DP $(r=0)$ and the PCPD point $(r=1)$.

Continuously varying critical exponents in nonequilibrium systems are very rare. Systems with infinitely many absorbing states like the PCP may display continuously varying exponents depending on initial conditions, but only the exponents describing nonstationary properties (δ' and η) are varying [13]. This variance is even disputed very recently [17,18]. Lévy-type long-range flights are known to be relevant to absorbing critical phenomena and the stationary critical exponents vary continuously with the exponent describing the long-range tail distribution of the flights [27]. However, the GPCPD involves only short-range processes. Recently, multispecies particle reaction-diffusion systems with interspecies hardcore interactions are conjectured to display continuously varying stationary-state exponents, but the transition occurs at the trivial annihilation point [28]. Moreover, the variance is very small and it would be extremely difficult to confirm it numerically. Our studies suggest strongly that the GPCPD belongs to a completely different type of universality class with continuously varying exponents which has not been explored before.

IV. UNIVERSALITY

In order to establish the universality class firmly, we study other model systems that share the common feature of the memory effect with the GPCPD. As described in Ref. [38], the PCPD can be regarded in a coarse-grained level as a cyclically coupled system of two particle species: one species A performing DP-like dynamics and the other species B performing the annihilating random walks. In the GPCPD model, a particle pair corresponds to an A particle and a solitary particle to a B particle. Two species are coupled through transmutations, which leads to the long-term memory effect. We set up two different 1D models of a cyclically coupled system and investigate numerically their scaling behavior to check our universality class. The two typical DP dynamics are employed for the A-particle dynamics, i.e. the branching-annihilating random walk model with one offspring (BAW1) [12] and the contact process.

The first model (referred to as the *ABB* model) adopts the BAW1 evolution rule for the A dynamics. Each lattice site is either occupied by an A or B particle, or empty. First, select a site at random. When it is occupied with an A, the A particle (a) branches an A with probability $(1-p)$ on a neighboring site, or (b) hops to a neighboring site with probability $p(1-\mu)$, or (c) transmutes to a B particle with probability $p\mu$. When the branched or hopping A particle lands on another A particle, both A particles annihilate immediately as in the BAW models. In case that it would land on a B particle, the trial is rejected and the B particle transmutes to the A particle. When the selected site is occupied with a B particle, the B particle hops to a neighboring site with probability d or does nothing with probability $1-d$. When it would land on another particle (either A or B), the trial is rejected and all involved B particles transmute to A particles. When the selected site is vacant, nothing happens.

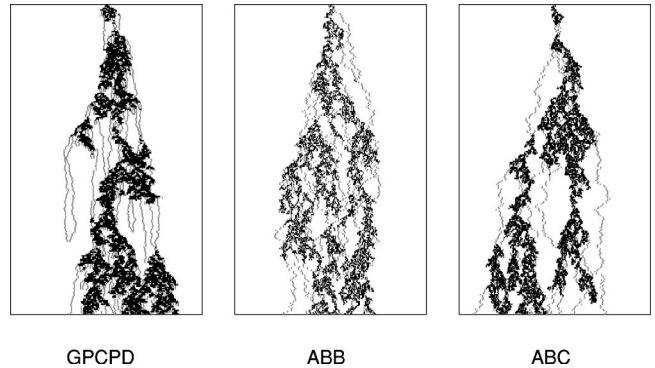

FIG. 8. Critical spreading of activities originated from a seed (a particle pair for the GPCPD and an A particle for the *ABB* and *ABC* models). A black pixel represents a particle pair or an A particle, and a gray one a solitary particle or a B particle. The horizontal [vertical (down)] direction corresponds to the space (time) direction.

The evolution rule of the second model (the *ABC* model) is almost equivalent to the *ABB* model, except that the contact process is adopted for the A particle dynamics. An A particle (a) branches an A with probability $(1-p)$ on a neighboring site, or (b) vanishes spontaneously with probability $p(1-\mu)$, or (c) transmutes to a B particle with probability $p\mu$. When the branched A particle would land on either A or B particle, the trial is rejected and the involved B particle transmutes to the A particle. A B particle hops to a neighboring site with probability d or does nothing with probability $1-d$, as in the ABB model. When it would land on another particle (either A or B), the trial is rejected and all involved B particles transmute to A particles.

In both models, the two species of particles are coupled cyclically through the transmutations. The transmutation rate from A to B is controlled explicitly by the parameter μ. As μ increases, the transmutation events occur more likely. At $\mu=0$, the $A\rightarrow B$ channel is completely blocked. Therefore there is no feedback mechanism to change the A particle density through intermediate B particles. The transmutation rate from B to A is implicit and determined by the evolution rule and the other control parameters. The $B\rightarrow A$ channel relies heavily on the diffusive property of B particles. With nonzero d, the B particles diffuse until they meet another particle and transmute to the A particles. This process invokes the same mechanism that gives rise to the long-term memory effect in the GPCPD model for $\mu\neq 0$. The B particles created by the A particles through transmutations perform the random walks before transmuting back to the A particles at later times. At $d=0$, the $B\rightarrow A$ channel is still open, but only with the short-term memory processes, which should be irrelevant.

We expect to observe the same type of critical behaviors, as in the GPCPD model, characterized by the continuously varying critical exponents. We performed the defect and static simulations to locate the critical points and estimate the critical exponents of the *ABB* and the *ABC* models at several values of μ with fixed hopping probability $d=1$. In Fig. 8, we compare the space-time structures of spreading patterns of activities in the GPCPD $(r=0.5)$, *ABB* $(\mu=0.5)$, and

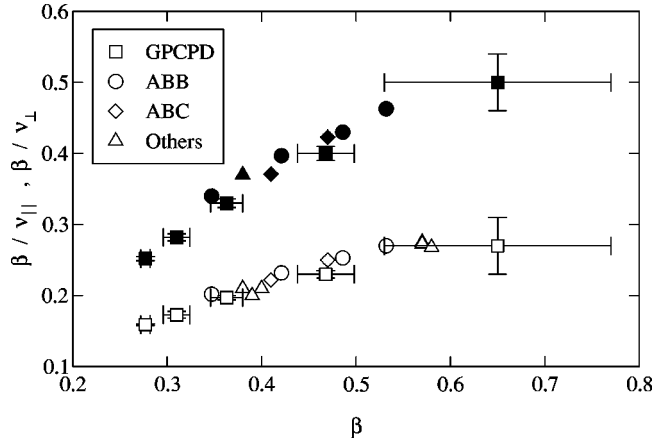

FIG. 9. Parametric plots of $\beta/\nu_\perp$ (filled symbol) and $\beta/\nu_\parallel$ (open symbol) with respect to β of the GPCPD, the *ABB*, and the *ABC* models. The data taken from Refs. [35,36,38–40] are also plotted and labeled by "Others."

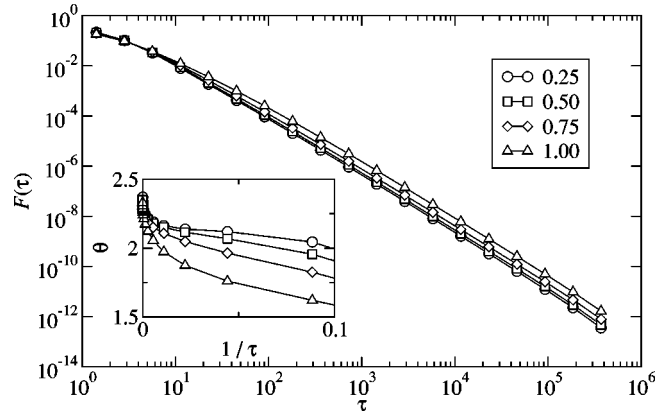

FIG. 10. Log-binned lifetime distribution of solitary particles at the critical points of the GPCPD with $r=0.25,\ldots,1.00$ and $t_{\max}=10^6$. Inset: Effective exponent for $F(\tau)\sim\tau^{-\theta}$. The apparent curvature near $\tau\simeq t_{\max}$ is simply due to the finite-$t_{\max}$ effect.

ABC ($\mu=0.2$) models at critical points. In all cases, the intermediate long-range diffusive processes of the solitary particles (or the *B* particles) are commonly observed between the particle pairs (or *A* particles) at different space-time positions. The time scale of these processes represents the effective *lifetime* of the intermediate *B* particles, which seems to be comparable to the simulation time. This aspect will be discussed quantitatively in the following section.

We take the *A* particle density as the order parameter and use the same definition of the surviving samples as in the GPCPD model, i.e. only the samples with at least one *A* particle are regarded as surviving ones. Here, we only state the results without showing the data. Our numerical simulations confirm that both *ABB* and *ABC* models show continuously varying exponents with the parameter μ. As expected, both models converge to the DP class at $\mu=0$.

In Fig. 9, the values of the critical exponents at various transmutation rates are plotted together with those for the GPCPD model and those available from other previous works [35,36,38–40]. Remarkably, they are lying along a single smooth line. It indicates that all these models fall into the same universality class with continuously varying exponents that can be parametrized by a single parameter (memory strength). The lines for $\beta/\nu_\perp$ and $\beta/\nu_\parallel$ seem to be almost linear for small $\beta<0.5$. It implies that the values of the correlation exponents, $\nu_\perp$ and $\nu_\parallel$, do not vary too much from the DP values, in contrast to a wide variation of the order parameter exponent β.

V. LIFETIME DISTRIBUTION OF INTERMEDIATE PARTICLES

Numerical results presented in the previous sections suggest that the critical exponents of the GPCPD model vary with the parameter *r* which controls memory strength. The memory effect is mediated by diffusing solitary particles. Each of them is created from a pair of two or more particles, diffuses until colliding with another particle, and then forms a particle pair with the probability *r*. Such a long-term process makes dynamics of the order parameter (pair density) nonlocal in time. In this section, we give a quantitative description of the long-term process by measuring the distribution of lifetime of intermediate solitary particles.

Simulations are performed up to $t\leqslant t_{\max}$ with a single particle pair (*A* particle) on an infinite lattice initially. Whenever an isolated particle (*B* particle) is created, a label recording the creation time is attached to it. Then, we can easily measure the *lifetime* of each isolated particle by recording the elapsed time until it collides with another particle since its creation (free diffusing time). We expect that the lifetime distribution $F(\tau)$ may be of the power-law type for large τ, because its long time tail should be governed by the annihilating random walk processes of solitary (*B*) particles in the presence of particle pairs (*A*).

At the critical points of the GPCPD model, the lifetime distribution $F(\tau)$ was measured with $t_{\max}=10^3,\ldots,10^6$. Figure 10 shows $F(\tau)$ averaged over 10^4 surviving samples with $t_{\max}=10^6$. We found that it follows power law asymptotically (large τ),

$$F(\tau)\sim\tau^{-\theta}. \tag{5}$$

The values of θ are determined from the effective exponent plots as shown in the inset. After the transient regime at small τ, the effective exponent converges to $\theta=2.25(5)$ at all values of *r*.

The distribution deviates from the power law when τ is comparable with the simulation time $t_{\max}$. At $t=t_{\max}$, there may exist remnant isolated particles whose lifetime can be comparable with or is larger than $t_{\max}$. The data of such isolated particles are not included in $F(\tau)$, which leads to a slight downward deviation of $F(\tau)$ for large $\tau\simeq t_{\max}$. Therefore, the apparent blowup of the effective exponent θ near $1/\tau=0$ in the inset of Fig. 10 should be ignored. The power-law distribution with $\theta=2.25(5)$ is observed universally for all three models considered in this paper. Note that the power-law distribution sets in later as one approaches the PCPD point at $r=1$. Presumably, this is related to the strong correction-to-scaling behavior observed in the PCPD.

For a more systematic analysis of the finite-$t_{\max}$ effect, we present in Fig. 11 the scaling plot of $F(\tau)t_{\max}^{2.25}$ versus $\tau/t_{\max}$.

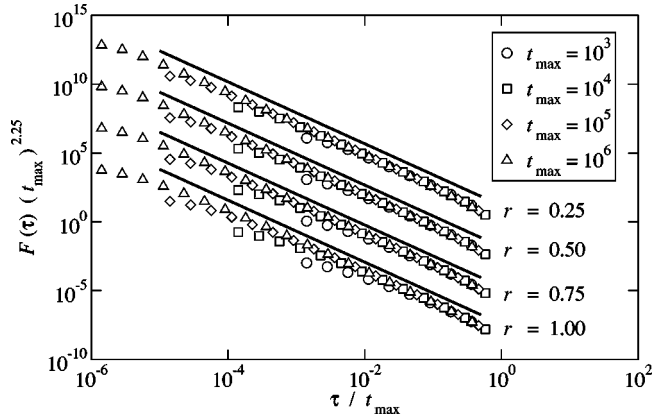

FIG. 11. Scaling plots of the log-binned lifetime distribution of solitary particles at the critical points of the GPCPD at $r=0.25,\ldots,1.00$. The straight lines have the slope 2.25. Each dataset at different values of r is shifted vertically by a constant factor to avoid overlaps.

The data collapse shows that the lifetime distribution follows the scaling relation $F(\tau)=t_{\max}^{-\theta}g_r(\tau/t_{\max})$ with $\theta=2.25$. The scaling function $g_r(x)$ should behave as $x^{-\theta}$ (independent of r) for small x, which is consistent with numerical data in Fig. 11.

The mean lifetime of the intermediate solitary particles, $\bar{\tau}\sim\int\tau F(\tau)d\tau$, is finite for $\theta>2$ and becomes infinite for $\theta\leqslant 2$. With finite lifetime, one may guess that the long-term memory effect can be washed away by rescaling the time by $\bar{\tau}$. Without the long term memory effect ($r=0$), the GPCPD displays the critical behavior in the DP class. Therefore, one may conclude that the presence of the intermediate particles and their long-term memory feedback are irrelevant and the GPCPD belongs to the DP universality class, regardless of the value of r. The exponent value $\theta=2.25$ is quite near the naively thought marginal value of $\theta_{\mathrm{mar}}=2$ where the mean lifetime $\bar{\tau}$ begins to diverge. With the DP scenario, one may argue that the apparent deviation of the critical exponents from the DP values is due to the strong corrections to scaling induced by quite large $\bar{\tau}$. However, a careful analysis for numerical data reveals that there are not much corrections to scaling for small r. Hence, this DP scenario does not seem to be supported by our present numerical results.

As an alternative, we propose another possible scenario to account for continuously varying non-DP exponents that the long-term memory effect plays the role of the marginal perturbation to the DP system. We note that the finiteness of the lifetime does not always guarantee the irrelevancy of the memory effects to the DP universality class in the fully interacting theory. The Lévy-flight DP system is such an example [27], where it is analytically shown by the ϵ-expansion-type RG analysis that the relevancy of long-range flights sets in a little bit earlier than expected from the naive noninteracting theory. It implies that the system flows into a non-DP fixed point with finite mean flight distance. We suspect that a similar situation also occurs in the GPCPD and θ_{mar} becomes slightly bigger than 2. In this point of view, our scenario may be still alive and even considered reasonable because $\theta=2.25(5)$ is not far away from 2. A definitive test on our scenario needs accurate determination of the marginal value in a full field-theoretical context, which is beyond the scope of the current paper.

VI. SUMMARY AND DISCUSSION

In summary, we introduced a generalized version of the PCPD (GPCPD) with a parameter controlling the long-term memory effect. The GPCPD connects the DP fixed point to the PCPD point continuously. We investigated numerically the nature of the absorbing phase transitions for the GPCPD in one dimension. Our numerical results strongly suggest that the GPCPD belongs to the universality class, which is characterized by the long-term memory effect and the continuously varying critical exponents. This model can be viewed as the cyclically coupled systems based on the DP dynamics with the long-term memory effect. We showed numerically that the two other variants of these systems fall into the same universality class.

We presented one possible scenario to account for this universality class that the intermediate particles generate the long-term memory effect which may play the role of the marginal operator to the DP fixed point. However, this is only speculative and definitely needs a full field-theoretical treatment.

Very recently, there have appeared several works on the PCPD and related models. Park and Kim [45] studied three different variants of the PCPD along a special line in the parameter space of the diffusion and the reaction rates. They found numerically that the exponent values for all three models are consistent within statistical errors, e.g., $\beta/\nu_{\parallel}\simeq 0.24(1)$. However, this does not imply that the PCPD scaling with general parameter values can be also described by the same fixed point.

Dickman and de Menezes [46] studied the PCPD using the same ensemble for the surviving samples as we used here. They found that this ensemble (called as the reactive sector) is quite useful to study the finite-size scaling of the order parameter. They observed numerically that the critical exponents vary with the diffusion rate d. Similar to our results, the correlation exponent $\nu_{\perp}$ appears to be independent of d and the same as the DP value. The relaxation time exponent $\nu_{\parallel}$ and the order parameter exponent β vary with d up to only about 20% (much smaller than the variation in the GPCPD $\sim 60\%$), which leads to an indecisive conclusion.

More recently, Hinrichsen [47] introduced a cellular automaton, which presumably belongs to the same universality class as the PCPD. Using a parallel update, he simulated the model with size up to $L=2^{21}$ until $t=2.5\times 10^6$. This work confirms again the difficulty in studying the critical behavior of the PCPD. The system does not reach the asymptotic scaling regime at that time scale. From the temporal trend of the effective exponents, he suggested an extremely slow crossover to DP, but this suggestion is also far from being conclusive. Recently, Barkema and Carlon [48] supported this scenario of an extremely slow crossover to DP by analyzing numerical data, assuming that the correction to scaling is of the special type. However, our numerical results for small r do not show this extremely slow crossover to DP as dis-

cussed in the preceding section.

Kockelkoren and Chaté [49] studied general reaction-diffusion processes without the fermionic constraint. From Monte Carlo study up to $L=2^{22}$ and $t\sim10^7$, they obtained $\beta/\nu_\parallel\simeq0.200$ in a model characterized with $XX\rightarrow XXX$ and $XX\rightarrow\varnothing$. They reported that the same exponents are observed in other similar models, and hence claimed that there is a single universality class for the PCPD. However, their study does not cover the general cases with controlling the memory effect. Ódor [50] studied the PCPD with Monte Carlo simulations up to $L=10^5$ and $t=10^8$, and obtained $\beta/\nu_\parallel\simeq0.21$ for high diffusion rates and $\beta/\nu_\parallel\simeq0.25$ for low diffusion rates. On the other hand, assuming a logarithmic correction, Ódor obtained $\beta/\nu_\parallel\simeq0.21$ also for the low diffusion rates.

These numerical results seem to favor a single non-DP universality class for the PCPD. However, as hinted in the work of Dickman and de Menezes [46], there may be, if any, a rather small variation ($<20\%$) of the scaling exponents by changing diffusion rates. So it is not surprising to see an apparent single universality under the effect of huge corrections to scaling. In contrast, the exponent variations in the GPCPD are much bigger ($\sim60\%$), so it is easier to confirm their variations.

We believe that the long-term memory effect is responsible for unusually long relaxation and non-DP scaling, and possibly for continuously varying exponents. The long-term memory is also present in the ordinary PCPD model, but it is controlled implicitly via diffusion rates d of isolated or intermediate particles. So, it may not be clear to predict how the long-term memory emerges with d. In the GPCPD model, we directly control the strength of the long-term memory effect by varying the parameter r.

The GPCPD model smoothly connects the DP fixed point ($r=0$) to the PCPD model ($r=1$), in a sense that the exponent values change with r continuously and monotonically, starting from the DP values. In contrast, the PCPD exponent values seem to jump from the DP values and decrease slightly with the diffusion rate d. For example, as soon as we turn on the diffusion process, $\beta/\nu_\parallel$ increases abruptly from the DP value of 0.1595 to ~0.25 at $d=0.1$ and slightly decreases to 0.20–0.23 at high $d=0.7$–0.8 [46,49,50]. Even if one accepts the claim that this variation is not real and $\beta/\nu_\parallel$ converges to ~0.20 asymptotically at any nonzero d (single universality class), one cannot avoid the fact that corrections to scaling are much bigger at low d than at high d. This suggests that the $d\rightarrow0$ limit in the PCPD model should encounter an unusual crossover behavior. In the ordinary crossover, one expects an interference of the DP fixed point on the PCPD universality class at $d\simeq0$, which generates an apparent exponent value between the DP and the PCPD value. All numerical results simply disagree with this. The apparent value (0.25) for $\beta/\nu_\parallel$ at low d is higher than both the DP (0.16) and the estimated PCPD value (0.20). Therefore, the $d=0$ limit in the PCPD model is unusually singular, which makes it impossible to study the PCPD scaling behavior systematically starting from the DP fixed point. In contrast, our GPCPD model is generically well suited to a systematic investigation of the PCPD model by controlling the long-term memory effect directly.

Besides that, there is one important technical point we adopted in this paper for analyzing the numerical data. As explained in Sec. III, we chose the *surviving* ensemble as the collection of samples with at least one particle pair and the order parameter as the particle pair density. With the conventional choice for the surviving ensemble (samples not trapped in one of the absorbing states), we found that the order parameter in finite-size systems bears two time scales (nontrivial relaxation time and trivial pair annihilation time) and does not show simple scaling collapse with one-variable scaling function like in Eq. (3) [44]. Our choice of the surviving sample should involve only one time scale and leads to an excellent scaling as shown in Fig. 6. With this ensemble, it is natural to choose the particle pair density (rather than the particle density) as the order parameter.

Summing up, we believe that the GPCPD model serves as an efficient generalized model to study the PCPD model systematically. The GPCPD seems to have much less corrections to scaling, compared to the ordinary PCPD model, which enables us to present accurate numerical data for the exponent values. In Figs. 2 and 4, one can clearly see that the asymptotic values for the exponents set in quite early, at around $t=10^3$, except the PCPD case ($r=1$). In order to check any possible long time crossover, we performed an extra static simulation for the GPCPD at $r=0.25$ on a lattice of size $L=4\times10^5$ up to $t=4\times10^7$. We found the more accurate critical point at $p_c=0.055\,045(3)$ and the exponent $\beta/\nu_\parallel\simeq0.172(2)$ [44]. The result is in excellent accord with our early-time result on a smaller lattice (see Tables I and II). This confirms again that the GPCPD for at least small r does not suffer from huge corrections to scaling as observed in Refs. [47,50]. However, for large $r=0.75$, we found that the exponent $\beta/\nu_\parallel$ tends to become smaller and seemingly approaches around 0.20 with $p_c=0.083\,11(1)$ in the very long time limit near $t\sim10^6$ [51]. So, at this stage, it is fair to say that the exponent $\beta/\nu_\parallel$ is not much sensitive to varying r for $r\geqslant0.5$, in contrast to the case for $r<0.5$.

ACKNOWLEDGMENTS

We thank P. Grassberger for his critical reading of this manuscript and valuable comments. We also thank H. Chaté for useful discussions, especially on the long time crossover for large r. This work was supported by Grant No. 2000-2-11200-002-3 from the Basic Research Program of KOSEF.

[1] For a review, see J. Marro and R. Dickman, *Nonequilibrium Phase Transitions in Lattice Models* (Cambridge University Press, Cambridge, 1999).

[2] H. Hinrichsen, Adv. Phys. **49**, 815 (2000).

[3] P. Grassberger, F. Krause, and T. von der Twer, J. Phys. A **17**, L105 (1984); P. Grassberger, *ibid.* **22**, L1103 (1989).

[4] H. Park and H. Park, Physica A **221**, 97 (1995).
[5] H. Hinrichsen, Phys. Rev. E **55**, 219 (1997).
[6] W. Hwang, S. Kwon, H. Park, and H. Park, Phys. Rev. E **57**, 6438 (1998).
[7] H.K. Janssen, Z. Phys. B **42**, 151 (1981).
[8] P. Grassberger, Z. Phys. B **47**, 365 (1982).
[9] T.E. Harris, Ann. Prob. **2**, 969 (1974).
[10] E. Domany and W. Kinzel, Phys. Rev. Lett. **53**, 311 (1984).
[11] R.M. Ziff, E. Gulari, and Y. Barshad, Phys. Rev. Lett. **56**, 2553 (1986).
[12] H. Takayasu and A.Yu. Tretyakov, Phys. Rev. Lett. **68**, 3060 (1992).
[13] I. Jensen, Phys. Rev. Lett. **70**, 1465 (1993); I. Jensen and R. Dickman, Phys. Rev. E **48**, 1710 (1993).
[14] G. Ódor, J.F. Mendes, M.A. Santos, and M.C. Marques, Phys. Rev. E **58**, 7020 (1998).
[15] J.F.F. Mendes, R. Dickman, M. Henkel, and M.C. Marques, J. Phys. A **27**, 3019 (1994).
[16] R. Dickman and D. ben-Avraham, Phys. Rev. E **64**, 020102 (2001).
[17] P. Grassberger, H. Chaté, and G. Rousseau, Phys. Rev. E **55**, 2488 (1997).
[18] A. Jiménez-Dalmaroni and H. Hinrichsen Phys. Rev. E **68**, 036103 (2003).
[19] F. van Wijland, Phys. Rev. Lett. **89**, 190602 (2002).
[20] N. Menyhárd, J. Phys. A **27**, 6139 (1994); N. Menyhárd and G. Ódor, *ibid.* **28**, 4505 (1995).
[21] M.H. Kim and H. Park, Phys. Rev. Lett. **73**, 2579 (1994); H. Park, M.H. Kim, and H. Park, Phys. Rev. E **52**, 5664 (1995).
[22] I. Jensen, Phys. Rev. E **50**, 3623 (1994).
[23] N. Inui and A.Yu. Tretyakov, Phys. Rev. Lett. **80**, 5148 (1998).
[24] W. Hwang and H. Park, Phys. Rev. E **59**, 4683 (1999).
[25] M.C. Marques and J.F.F. Mendes, Eur. Phys. J. B **12**, 123 (1999).
[26] H.S. Park and H. Park, J. Korean Phys. Soc. **38**, 494 (2001).
[27] H.K. Janssen, K. Oerding, F. van Wijland, and H.J. Hilhorst, Eur. Phys. J. B **7**, 137 (1999); H. Hinrichsen and M. Howard, *ibid.* **7**, 635 (1999).
[28] S. Kwon, J. Lee, and H. Park, Phys. Rev. Lett. **85**, 1682 (2000).
[29] M. Rossi, R. Pastor-Satorras, and A. Vespignani, Phys. Rev. Lett. **85**, 1803 (2000).
[30] A. Lipowski and M. Droz, Phys. Rev. E **65**, 056114 (2002).
[31] A.J. Noest, Phys. Rev. Lett. **57**, 90 (1986); M. Bramson, R. Durrett, and R.H. Schönmann, Ann. Prob. **19**, 960 (1991); A.G. Moreira and R. Dickman, Phys. Rev. E **54**, R3090 (1996); R. Cafiero, A. Gabrielli, and M. Muñoz, *ibid.* **57**, 5060 (1998); J. Hooyberghs, F. Iglói, and C. Vanderzande, Phys. Rev. Lett. **90**, 100601 (2003).
[32] A binary spreading process such as the PCPD was first introduced and studied by Grassberger in Ref. [8].
[33] M.J. Howard and U.C. Täuber, J. Phys. A **30**, 7721 (1997).
[34] E. Carlon, M. Henkel, and U. Schollwöck, Phys. Rev. E **63**, 036101 (2001).
[35] H. Hinrichsen, Phys. Rev. E **63**, 036102 (2001).
[36] G. Ódor, Phys. Rev. E **62**, R3027 (2000).
[37] H. Chaté and P. Grassberger (unpublished).
[38] H. Hinrichsen, Physica A **291**, 275 (2001).
[39] K. Park, H. Hinrichsen, and I.-M. Kim, Phys. Rev. E **63**, 065103 (2001).
[40] G. Ódor, Phys. Rev. E **63**, 067104 (2001).
[41] This trivial dynamics may be "dressed" by the interference with the local clouds of particle pairs. This issue will be discussed elsewhere.
[42] P. Grassberger and A. De La Torre, Ann. Phys. (N.Y.) **122**, 373 (1979).
[43] It does not imply that the estimate using the plot of $\delta'(t)$ or $z(t)$ versus $1/t$ would yield a different value of p_c. In such cases the upward and downward curvature at off-critical points guides the estimation, which leads to the same result.
[44] J. D. Noh and H. Park (unpublished).
[45] K. Park and I.-M. Kim, Phys. Rev. E **66**, 027106 (2002).
[46] R. Dickman and M.A.F. de Menezes, Phys. Rev. E **66**, 045101(R) (2002).
[47] H. Hinrichsen, Physica A **320**, 249 (2003).
[48] G.T. Barkema and E. Carlon, Phys. Rev. E **68**, 036113 (2003).
[49] J. Kockelkoren and H. Chaté, Phys. Rev. Lett. **90**, 125701 (2003).
[50] G. Ódor, Phys. Rev. E **67**, 067104 (2003).
[51] This was first pointed out by H. Chaté (private communication).